

## Potassium incorporation-induced modification of electrical properties of ZnO nanorods and its application to piezoelectric nanogenerators

Il-Kyu Park\*

Department of Materials Science and Engineering, Seoul National University of Science and Technology, Seoul 139-743, South Korea

In this study, the modification of the electrical properties of ZnO nanorods (NRs) was investigated by incorporating potassium (K) during a hydrothermal process. Structural investigations reveal that the K incorporation improved the crystalline quality of the ZnO NRs with a negligible change in the morphology. The electrical properties of the ZnO NR/*p*-Si heterojunction indicated a gradual elimination of defect-induced free charge carriers by the incorporation of K element. A piezoelectric nanogenerator was fabricated using the K incorporated ZnO NRs, which showed enhanced piezoelectric output potential due to the elimination of the screening effect by free charge carriers in the NRs.

**Key words:** ZnO nanorod, Hydrothermal, Doping, Piezoelectric, Nanogenerator.

### Introduction

ZnO material systems have attracted much attention due to their excellent physical properties, including a wide bandgap in the near-UV spectral range, large exciton binding energy (60 meV), large piezoelectric and pyroelectric coefficient properties, and easy fabrication of nanostructures with various shapes [1-3]. However, it is difficult to control the electrical properties of ZnO, which has hindered the application of ZnO as a semiconductor in electronic or optoelectronic devices. Theoretical investigations based on first principles and density functional theory have shown that ZnO materials have unintentional *n*-type conductivity due to abundant native point defects and impurities [4]. Therefore, it is easy to fabricate *n*-type doped ZnO, but it has remained challenging to achieve reproducible and stable doping with an acceptor for *p*-type conductivity in ZnO.

To overcome this problem, many strategies have been attempted to obtain *p*-type conductivity in ZnO materials by incorporating various elements and using various synthesis methods, such as physical vapor deposition, thermal vapor transport methods, hydrothermal methods, and spin-on dopant methods [5-9]. Much improvement has been achieved for ZnO materials, but it is still difficult to control the electrical properties of ZnO nanorod (NR) structures. Furthermore, they require complicated techniques and high-temperature processes [5-9]. Therefore, a new dopant is needed to control the

electrical properties of ZnO NRs.

In particular, group I alkaline elements have been considered as effective *p*-type dopants due to the possibility of endohedral doping in ZnO cage-like materials [10]. For example, Li and Na have been used to obtain *p*-ZnO nanomaterials [11, 12]. However, there has been no report on the use of K, another group I element, for controlling the electrical properties of ZnO materials. In this study, we successfully modified the electrical properties of ZnO NRs by incorporating K during a solution-based hydrothermal growth process. We also investigated the beneficial effects by using the ZnO NRs to fabricate piezoelectric nanogenerators (PNGs).

### Experimental Procedure

K-incorporated ZnO NRs were grown on an *n*- and *p*-type Si (100) wafers by a two-step hydrothermal method consisting of seed layer formation and ZnO NR growth [13]. Fig. 1 shows the fabrication process of the K-incorporated ZnO NRs and PNG devices. The substrate was cleaned by a conventional method to remove surface contaminations by using acetone, methanol, and deionized (DI) water in ultrasonic bath each for 5 min. The ZnO NRs, ZnO seed layer was formed by dipping the Si substrate into a mixed solution of 60 mM zinc acetate dihydrate ( $Zn(CH_3COO)_2 \cdot 2H_2O$ ) dissolved in ethanol at 80 °C for 1 min, followed by drying on a hot plate at 100 °C for 5 min. The K-incorporated ZnO NRs were then grown at 90 °C for 3 hrs in a mixed solution of 60 mM zinc nitrate hexahydrate ( $Zn(NO_3)_2 \cdot 6H_2O$ ), 60 mM hexamethylenetetramine ( $(CH_2)_6N_4$ ; HMT), and various concentrations of potassium nitrate ( $K(NO_3)$ ) dissolved in DI water. The amount of the K source was

\*Corresponding author:  
Tel : +82-2-970-6349  
Fax: +82-2-973-6657  
E-mail: pik@seoultech.ac.kr

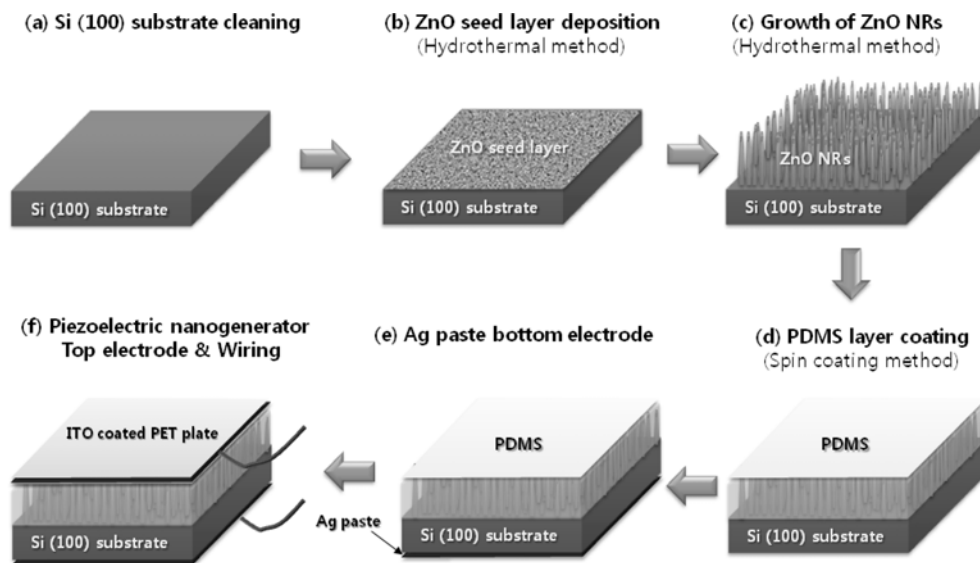


**Fig. 1.** Schematic of processing steps for fabricating K-incorporated ZnO NRs and ZnO-based PNG devices.

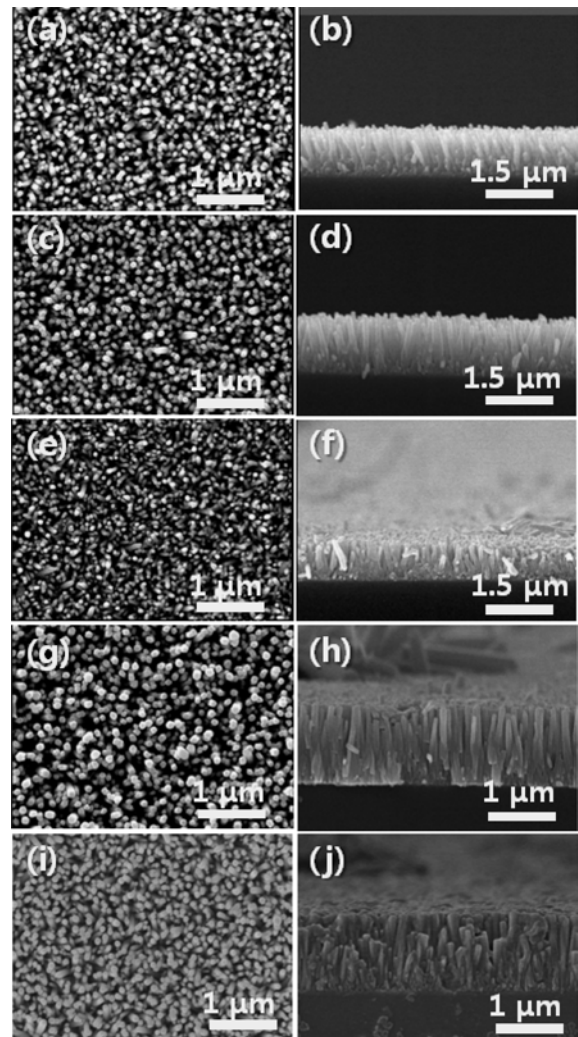
varied from 0 to 30% of the molarity of the Zn source. Even with 30% of the K source, it dissolved completely and resulted in a clear solution. After the reaction, the samples were cleaned with DI water in an ultrasonic bath for 5 min to completely remove the homogeneously formed ZnO nanostructures, which have a detrimental effect on the device performance.

The structure and morphology of the K-incorporated ZnO NRs were observed by field emission scanning electron microscopy (FE-SEM). Crystallographic information about the NRs was obtained by high-resolution X-ray diffraction (HR-XRD). The electrical properties were investigated using a source meter (Keithley-2400). An oscilloscope (TBS1202B, Tektronix) was used to measure the piezoelectric output voltage from the PNGs by applying periodic compressive stress.

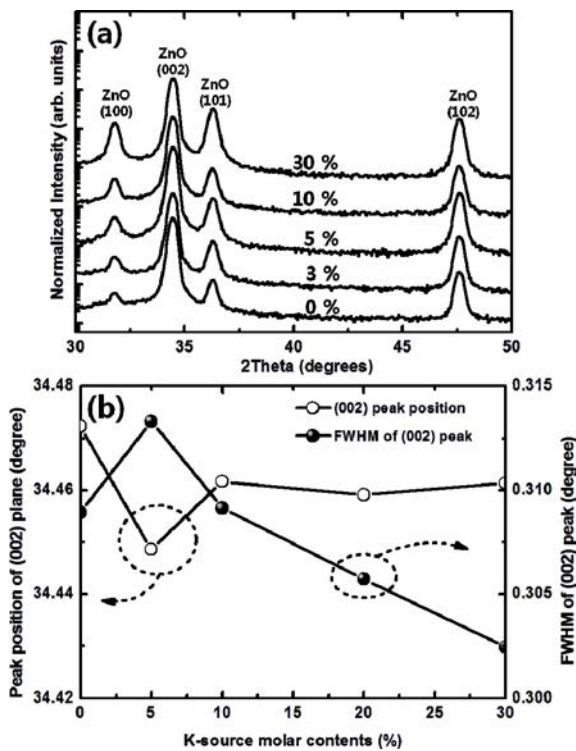
## Results and Discussion

Fig. 2 shows the surface morphology and cross-sectional structure of undoped and K-incorporated ZnO NRs. As shown in Figs. 2(a) and (b), the diameter and length of the undoped ZnO NRs were around 60–80 nm and 960 nm, respectively, and the shapes were uniform. The ZnO NRs were closely packed with density greater than  $10^{10}/\text{cm}^2$  due to the densely formed ZnO nucleation seed layer. Even with 30% of the K source, the morphology of the ZnO NRs showed negligible change. This indicates that the K source did not significantly affect the growth mechanism.

The crystalline properties of ZnO NRs were investigated by the HR-XRD as shown in Fig. 3(a). All samples showed four main peaks corresponding to the (100), (002), (101), and (102) planes of the hexagonal ZnO crystal. These patterns matched well with those of bulk ZnO with wurtzite structure (space group: P63mc;  $a = 0.0.32501$  nm,  $c = 0.52071$  nm, JCPDS 79-2205).



**Fig. 2.** Plan view and cross-sectional view FE-SEM images of (a) and (b) undoped (0%); (c) and (d) 5% K-incorporated; (e) and (f) 10% K-incorporated; (g) and (h) 20% K-incorporated; and (i) and (j) 30% K-incorporated ZnO NRs, respectively.



**Fig. 3.** (a) Normalized  $\theta$ -2 $\theta$  XRD patterns of undoped and K-incorporated ZnO NRs with variation of the K source concentrations in the solution. (b) Variation of ZnO (002) peak position with variation of the K-source concentration. (c) FWHM of (002) and (102) diffraction peaks with variation of K source molar contents in the solution.

No additional peaks were found in the diffraction results, indicating that unintentional chemical species were not formed, such as K-related oxides or metallic compounds.

To investigate more about the variation of crystalline properties of ZnO NRs, the (002) peak position and its full-width at half maximum (FWHM) were plotted for various K source contents. As the K content increased, the (002) diffraction peaks shifted slightly to lower angles. According to Bragg's law for X-ray diffraction, this indicates an increment of the lattice size with the incorporation of K ions into the ZnO lattice. Because of the larger ionic radius of the  $K^+$  (1.33 Å) ion than  $Zn^{2+}$  (0.74 Å), the inter-atomic distance of the (002) plane increases as the  $K^+$  ions substitute for the  $Zn^{2+}$  sites in the crystal lattice. Even 30% K-source content, the peak did not shift any further due to the large difference in the ionic radius of  $K^+$  and  $Zn^{2+}$  ions. A large difference in the ionic radius of a foreign atom and a matrix atom can hinder the incorporation. However, the FWHM of the (002) peak decreased gradually after the sudden increase for the 5% sample. The FWHM for the diffraction peak implies the relative quantity of the crystalline defects contained in the crystal lattice [13]. Therefore, a decrease in the FWHM indicates that crystal defects, such as vacancies, interstitial atoms, and various dislocations

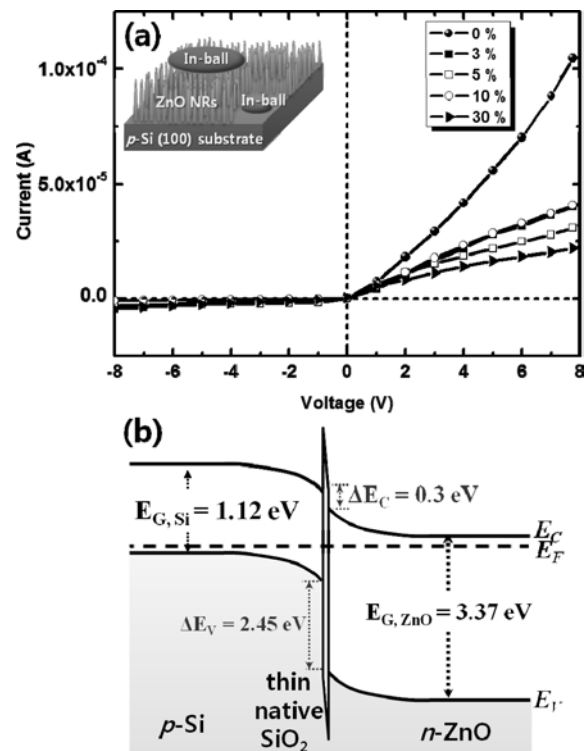
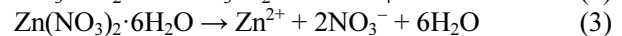
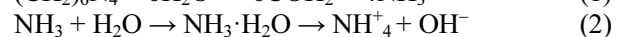


**Fig. 4.** (a) I-V characteristics of the K-incorporated ZnO NR/*p*-Si heterojunctions with variation of the K source molar contents in the solution. The inset shows a schematic view of a heterojunction structure. (b) Equilibrium energy band diagram for the *n*-ZnO/*p*-Si heterojunction.

can be reduced by increasing the K source contents. The ionic radius of the  $K^+$  ion is about 1.8 times larger than that of  $Zn^{2+}$  ions. Therefore, a large amount of  $K^+$  ions cannot be incorporated into the ZnO lattice, but they can be incorporated slightly by substituting into the Zn lattice sites and vacancy sites. Thus the K-incorporation can affect the growth of ZnO NRs. The hydrothermal chemical reactions for the K incorporated ZnO NRs growth can be summarized by the following reactions:



Based on these chemical reactions, the  $K^+$  ions can be incorporated into sites of the ZnO crystal lattice.

Fig. 4(a) shows the current-voltage (I-V) characteristics for the ZnO NRs/*p*-Si heterojunction structures, which were used to investigate the electrical properties of the NRs. As shown in the inset of Fig. 4(a), a commercial precision solder sphere (an indium-ball with a diameter of 300  $\mu$ m) was used as a contact material for the ZnO NRs and *p*-Si [14]. The defect-induced unintentionally doped *n*-ZnO NR/*p*-Si heterojunction showed rectifying

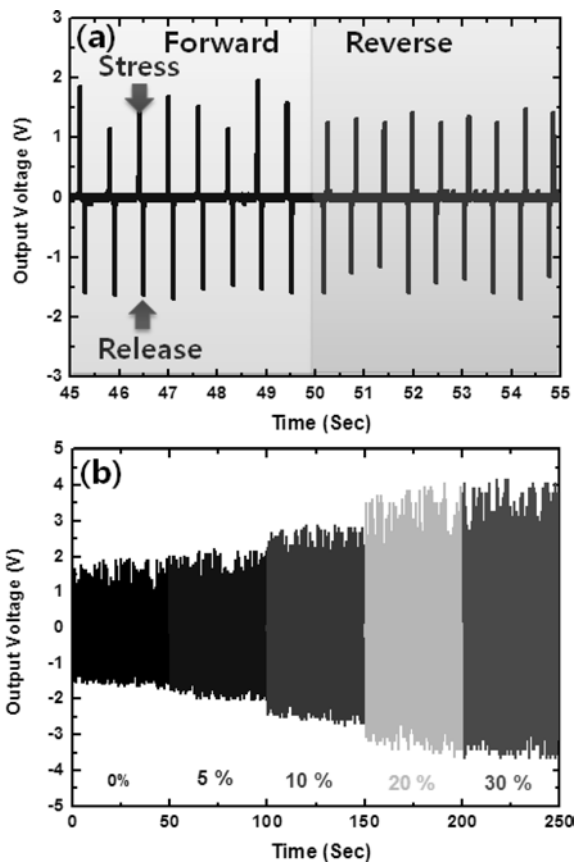


**Fig. 5.** (a) Polarity-dependent output voltage for a PNG fabricated using undoped ZnO NRs. (b) Output voltage measured from the K-incorporated ZnO NR-based PNGs with variation of the K source molar contents in the solution.

behavior. Undoped ZnO NRs grown via a solution-based hydrothermal method usually contain various point defects, such as oxygen vacancies, zinc interstitials, and their complexes, which can result in intrinsic *n*-type behavior. Thus, a heterojunction consisting of the undoped NR and *p*-Si forms a rectifying junction, as shown in Fig. 4(b). The equilibrium energy band diagrams were obtained using the Anderson model [15] and band parameters of  $E_g$  (ZnO) = 3.37 eV,  $\chi$  (ZnO) = 4.35 eV [16],  $E_g$  (Si) = 1.12 eV [17], and  $\chi$  (Si) = 4.05 eV [18]. At the junction between the substrate and ZnO NRs, a thin oxide layer inevitably forms on the Si surface during dipping in the hydrothermal solution [19]. With increasing molar contents of the K source, the forward current decreases gradually. This is attributed to the decrease in free charge carriers in the ZnO NRs due to compensation by the K ions, which act as acceptors in the crystal lattice. At the same time, K incorporation can reduce the point defects as described above. Therefore, the extinction of the intrinsic electrical charge carriers by the K incorporation results in an increase of the electrical resistance of the ZnO NRs. These results indicate that the K incorporation can successfully reduce the free charge carriers and modify the electrical properties of the NRs.

To confirm the beneficial effect of the K incorporation into ZnO NRs, we demonstrated a PNG by attaching an ITO-coated polyethylene terephthalate (PET) plate to the NRs as a top electrode, as shown in Fig. 1(f) [20]. Fig. 5(a) shows the polarity switching test of the PNG devices using undoped ZnO NRs, which was performed to determine the origin of the measured signals. The PNG devices were connected in the forward and reverse directions. A forward connection means that the positive probe of the measurement system is connected to the top ITO electrode, and negative probe is connected to the back Ag electrode of the Si substrate. As shown in Fig. 5(a), a periodic sequence of positive and negative voltage peaks occurs when the PNGs are pushed and released, resulting in charging and discharging, respectively. When a piezoelectric ZnO NR is subjected to a compressive stress, a piezoelectric potential is generated along the NRs due to the relative displacement of cations with respect to the anions under uniaxial strain. These results indicate that the output signals are generated by the PNG itself rather than the measurement system.

Fig. 5(b) shows the time-dependent piezoelectric output potential from the PNGs for various K contents. As the K content increases, the piezoelectric output potential also increases gradually. The piezoelectric potential generated in the individual ZnO NRs under external strain can be expressed as  $\varphi_{max} = |F_V| \gamma_V \frac{L}{\pi R^2}$ , where  $F_V$ ,  $R$ , and  $L$  are the applied force, radius, and length of the ZnO NR, respectively [21]. And  $\gamma_V$  is a material parameter that affects the potential generated according to the strain magnitude. Therefore, if the shape and displacement of each ZnO NR are the same, the piezoelectric potential generated from the individual ZnO NRs can be affected by the  $\gamma_V$  value. This value depends on the concentration of free charge carriers. Usually, reducing the free charge carriers in piezoelectric active materials is known to enhance the piezoelectric output because they screen the generated piezoelectric potential [22]. The free charge carriers induced by defects in the ZnO NRs were decreased with increasing K source contents, which can enhance the performance of ZnO NR-based nanogenerators. In addition, the method is simple, cost-effective, and expandable for producing semiconducting materials and could broaden their potential applications.

## Conclusions

In summary, we have successfully modified the electrical properties of ZnO NRs by incorporating K. The K-incorporated ZnO NRs did not show a significant change in morphology, even when the K content was increased to 30%. The crystal quality of the ZnO NRs measured by HR-XRD showed improvement

with increasing K contents. The electrical properties of the ZnO NR/p-Si heterojunction showed that the defect-induced free charge carriers were reduced as K was incorporated. Because of these effects, the PNGs fabricated using the ZnO NRs showed enhanced piezoelectric output potential with increasing K molar content. The enhanced piezoelectric output was attributed to the elimination of the screening effect by free charge carriers in the NRs. This approach provides a simple and cost-effective doping method for ZnO material systems, as well as enhanced performance for energy conversion devices based on ZnO NRs.

### Acknowledgments

The author especially thanks to Mr. Gwang-Hee Nam (Yeungnam University) for assistance with the experiments. This study was supported by the Basic Science Research Program (NRF-2014R1A2A1A11054154) through the National Research Foundation of Korea funded by the Ministry of Science, ICT and Future Planning of the Korean government.

### References

1. A. Janotti and C.G.V. Walle, *Rep. Prog. Phys.* 72 (2009) 126501-126530.
2. A. Umar and Y.B. Hahn, in "Metal oxide nanostructures and their applications: ZnO nanostructures and Nanodevices" (American Scientific Publishers, 2010), pp. 2-107.
3. J.H. Koo and B.W. Lee, *J. Ceram. Process. Res.* 18 (2017) 156-160.
4. C.G.V. Walle, *Phys. Rev. Lett.* 85 (2000) 1012-1015.
5. D.C. Look, *Mater. Sci. Eng. B* 80 (2001) 383-387.
6. J.H. Lim, C.K. Kang, K.K. Kim, I.K. Park, and S.J. Park, *Adv. Mater.* 18 (2006) 2720-2724.
7. S. Chu, G. Wang, W. Zhou, Y. Lin, L. Chernyak, J. Zhao, J. Kong, L. Li, J. Ren, and J. Liu, *Nature Nanotech.* 6 (2011) 506-510.
8. K.K. Kim and I.K. Park, *J. Ceram. Process. Res.* (accepted).
9. J.I. Sohn, Y.-I. Jung, S.-H. Baek, S. Cha, J. E. Jang, C.-H. Cho, J.H. Kim, J.M. Kim, and I.K. Park, *Nanoscale*, 6 (2014) 2046-2051.
10. D. Hapiuk, M.A.L. Marques, P. Melinon, J.A. Flores-Livas, S. Botti, and B. Masenelli, *Phys. Rev. Lett.*, 108 (2012) 115903.
11. W. Liu, F. Xiu, K. Sun, Y. H. Xie, K. L. Wang, Y. Wang, J. Zou, Z. Yang, and J. Liu, *J. Am. Chem. Soc.* 132 (2010) 2498-2499.
12. J.S. Lee, S.N. Cha, J.M. Kim, H.W. Nam, S.H. Lee, W.B. Ko, K.L. Wang, J.G. Park, and J.P. Hong, *Adv. Mater.*, 23 (2011) 4183-4187.
13. Y.S. Lee, S.N. Lee, and I.K. Park, *Ceramics International* 39 (2013) 3043-3048.
14. S. Singh, I.K. Park, and S.H. Park, *J. Ceram. Process. Res.* 17 (2016) 218-222.
15. R.L. Anderson, *Solid-State Electron.* 5 (1962) 341-344.
16. C.H. Ahn, Y.Y. Kim, D.C. Kim, S.K. Mohanta, and H.K. Cho, *J. Appl. Phys.* 105 (2009) 013502.
17. C. Wu, X. Qiao, L. Luo, and H. Li, *Mater. Res. Bull.* 43 (2009) 1883-1891.
18. J.A. Aranovich, D.G. Golmayo, A.L. Fahrenbruch, and R.H. Bube, *J. Appl. Phys.* 51 (1980) 4260-4268.
19. I.S. Jeong, J.H. Kim, and S. Lim, *Appl. Phys. Lett.* 83 (2003) 2946-2948.
20. M. Ahmad, M.A. Iqbal, J. Kiely, R. Luxton, M. Jabeen, *J. Phys. Chem. Solids* 104 (2017) 281-285.
21. G. Romano, G. Mantini, A.D. Carlo, A.D'Amico, C. Falconi, and Z.L. Wang, *Nanotechnology* 22 (2011) 465401.
22. J.I. Sohn, S.N. Cha, B.G. Song, S. Lee, S.M. Kim, J. Ku, H.J. Kim, Y.J. Park, B.L. Choi, Z.L. Wang, J.M. Kim, and K. Kim, *Energy Environ. Sci.* 6 (2013) 97-104.